AD-A100 238 ROME AIR DEVELOPMENT CENTER GRIFFISS AFB NY F/G 20/14
MF RADIO FIELD STRENGTH MEASUREMENTS IN DESERT TERRAIN NEAR YUM--ETC(U)
DEC 80 J L HECKSCHER, C B KALAKOWSKY
UNCLASSIFIED RADC-TR-80-359 NL

1 of 1
AD
A100238

END
DATE
FILMED
7-81
DTIC

LEVEL II (12)

RADC-TR-80-359
In-House Report
December 1980

MF RADIO FIELD STRENGTH MEASUREMENTS IN DESERT TERRAIN NEAR YUMA, ARIZONA

John L. Heckscher
Charles B. Kalakowsky
Roger W. Whidden
Eli J. Tichovolsky

APPROVED FOR PUBLIC RELEASE; DISTRIBUTION UNLIMITED

ROME AIR DEVELOPMENT CENTER
Air Force Systems Command
Griffiss Air Force Base, New York 13441

This report has been reviewed by the RADC Public Affairs Office (PA) and is releasable to the National Technical Information Service (NTIS). At NTIS it will be releasable to the general public, including foreign nations.

RADC-TR-80-359 has been reviewed and is approved for publication.

APPROVED:

TERENCE J. ELKINS, Acting Chief
Propagation Branch
Electromagnetic Sciences Division

APPROVED:

ALLAN C. SCHELL, Chief
Electromagnetic Sciences Division

FOR THE COMMANDER:

JOHN P. HUSS
Acting Chief, Plans Office

Unclassified

SECURITY CLASSIFICATION OF THIS PAGE (When Data Entered)

REPORT DOCUMENTATION PAGE		READ INSTRUCTIONS BEFORE COMPLETING FORM
1. REPORT NUMBER RADC-TR-80-359	2. GOVT ACCESSION NO. AD-A100 238	3. RECIPIENT'S CATALOG NUMBER
4. TITLE (and Subtitle) MF RADIO FIELD STRENGTH MEASUREMENTS IN DESERT TERRAIN NEAR YUMA, ARIZONA		5. TYPE OF REPORT & PERIOD COVERED In-house
		6. PERFORMING ORG. REPORT NUMBER
7. AUTHOR(s) John L. Heckscher, Roger W. Whidden, Charles B. Kalakowsky, Eli J. Tichovolsky*		8. CONTRACT OR GRANT NUMBER(s)
9. PERFORMING ORGANIZATION NAME AND ADDRESS Deputy for Electronic Technology (RADC/EEP) Hanscom AFB Massachusetts 01731		10. PROGRAM ELEMENT, PROJECT, TASK AREA & WORK UNIT NUMBERS 62702F 46001606
11. CONTROLLING OFFICE NAME AND ADDRESS Deputy for Electronic Technology (RADC/EEP) Hanscom AFB Massachusetts 01731		12. REPORT DATE July 1980
		13. NUMBER OF PAGES 20
14. MONITORING AGENCY NAME & ADDRESS(if different from Controlling Office)		15. SECURITY CLASS. (of this report) Unclassified
		15a. DECLASSIFICATION DOWNGRADING SCHEDULE

16. DISTRIBUTION STATEMENT (of this Report)

Approved for public release; distribution unlimited.

17. DISTRIBUTION ST ENT (of abstract entered in Block 20, if different from Report)

18. SUPPLEMENTARY TES

*Arcon Corp., Waltham, Massachusetts 02154

19. KEY WORDS (Continue on reverse side if necessary and identify by block number)

MF propagation
MF ground wave
MF radio field strength

20. ABSTRACT (Continue on reverse side if necessary and identify by block number)

The field strength of the commercial radio broadcast station KBLU was measured at several hundred locations in the desert southeast of Yuma, Arizona, to study MF ground-wave propagation over the desert valleys and mountain ridges. Field strengths below the surface of the desert floor were measured in specially drilled holes to observe the penetration of MF into the desert soil. Idealized propagation path models are shown to produce effects similar to the observations.

DD FORM 1 JAN 73 1473

Unclassified

SECURITY CLASSIFICATION OF THIS PAGE (When Data Entered)

Preface

We appreciate the valuable suggestions, helpful information, and willing cooperation of the many individuals who contributed to this effort. In particular, we are indebted to Dr. Edward A. Lewis, Chief, Propagation Branch RADC/EEP, for suggesting the technique for measuring radio wave penetration of soil; to Robert Crites, Manager, and Richard Nix, Chief Engineer, both of KBLU Radio, Yuma for supplying station logs and field strength measurements which were extremely useful in the data reduction; and to James T. Neal, Lt. Col., USAF, Chief, Special Projects Office, Civil Engineering Research Division, AFWL for kindly arranging field support services at the HAVE HOST site. We also thank Wayne I. Klemetti for his able assistance in preparing the illustrations.

This work was performed at the request of the Space and Missile Systems Organization (SAMSO) under the sponsorship of Robert Barberg, Capt, USAF, SAMSO/MNNL and the technical direction of Mr. Jim Culhane, TRW.

Contents

Illustrations

Illustrations

Tables

MF Radio Field Strength Measurements in Desert Terrain Near Yuma, Arizona

1. INTRODUCTION

The possibility that a network of underground tunnels or silos containing the MX mobile missile might be constructed in the desert regions of the southwestern United States has renewed interest in techniques for survivable communications between buried terminals which may be up to 50 km apart in adjacent valleys separated by high mountain ridges. One proposed method is to use an MF radio link with the transmitting and receiving antennas located on the underground mobile launch control centers. The propagation path for such a link would include two segments through the trench wall and soil overburden in addition to that over the desert terrain. Although MF propagation curves over homogeneous earth are readily available,[1-4] propagation anomalies caused by topographical and electrical irregularities unique to the proposed MX sites need to be studied in situ.

(Received for publication 24 November 1980)

1. Terman, F. E. (1943) Radio Engineer's Handbook, McGraw-Hill, New York.
2. Wait, J. R., and Campbell, L. L. (1953) Transmission curves for ground wave propagation at low radio frequencies, Radio Physics Laboratory Report R-1, Defence Research Telecommunications Establishment, Ottawa.
3. International Radio Consultative Committee (C. C. I. R.) (1974) Propagation in Non-Ionized Media (Study Group 5), Vol. 5, XIIIth Plenary Assembly, Geneva, 1974, International Telecommunication Union, Geneva, 1975.
4. Reference Data for Radio Engineers, 4th ed. (1956) ITT Corp., New York, p. 714 ff.

2. EXPERIMENTAL PROCEDURE

Between 11 September and 24 September 1977 personnel from Rome Air Development Center (RADC/EEP) made field strength measurements of the Yuma, Arizona broadcast station KBLU (560 kHz, 1 kW, omni-directional in the daytime) at several hundred positions on Luke AF Bombing and Gunnery Range, a desert region southeast of Yuma. At each site the surface magnetic field was measured using a Radio Interference-Field Intensity Measuring Equipment, Singer Model NM-25T, with a shielded 15-in. -diameter loop antenna oriented for maximum signal. At some of the sites the loop also was lowered 2 m into a hole drilled by a power auger to probe the radio wave attenuation with depth. The measurements were conducted only during daylight hours to eliminate the necessity of correcting for KBLU day-to-night antenna pattern changes and to minimize sky wave interference.

The measurement sites were accurately located in almost every case by choosing positions near the numerous USGS markers found alongside Jeep trails. The sites are shown in Figure 1, along with the location of the KBLU transmitting antenna in downtown Yuma. The distribution of the markers was such that no series of measurements was strictly aligned along a radial path from KBLU. However, six sectors were chosen within which the terrain could be characterized reasonably well by a single profile, thus providing a convenient way to group and display the data. Dashed lines are used in Figure 1 to show the sector boundaries. A representative path profile, corrected for the standard tropospheric refractive index gradient[5] (4/3 earth radius), was constructed for each sector using USGS maps.

3. FLAT EARTH PROPAGATION THEORY

Over a flat, homogeneous, and well-conducting earth the vertical electric field strength-distance product is given by

$$|E \cdot x| = 300\sqrt{P} \cdot |F(p_e)| \text{ (Volts)} \tag{1}$$

where P is the effective radiated power in kW,

$$F(p_e) = 1 - i\sqrt{\pi p_e} \cdot e^{-p_e} \cdot \operatorname{erfc}(i\sqrt{p_e})$$

5. Reference Data for Radio Engineers, 5th ed., (1957) ITT Corp., New York p 741 ff.

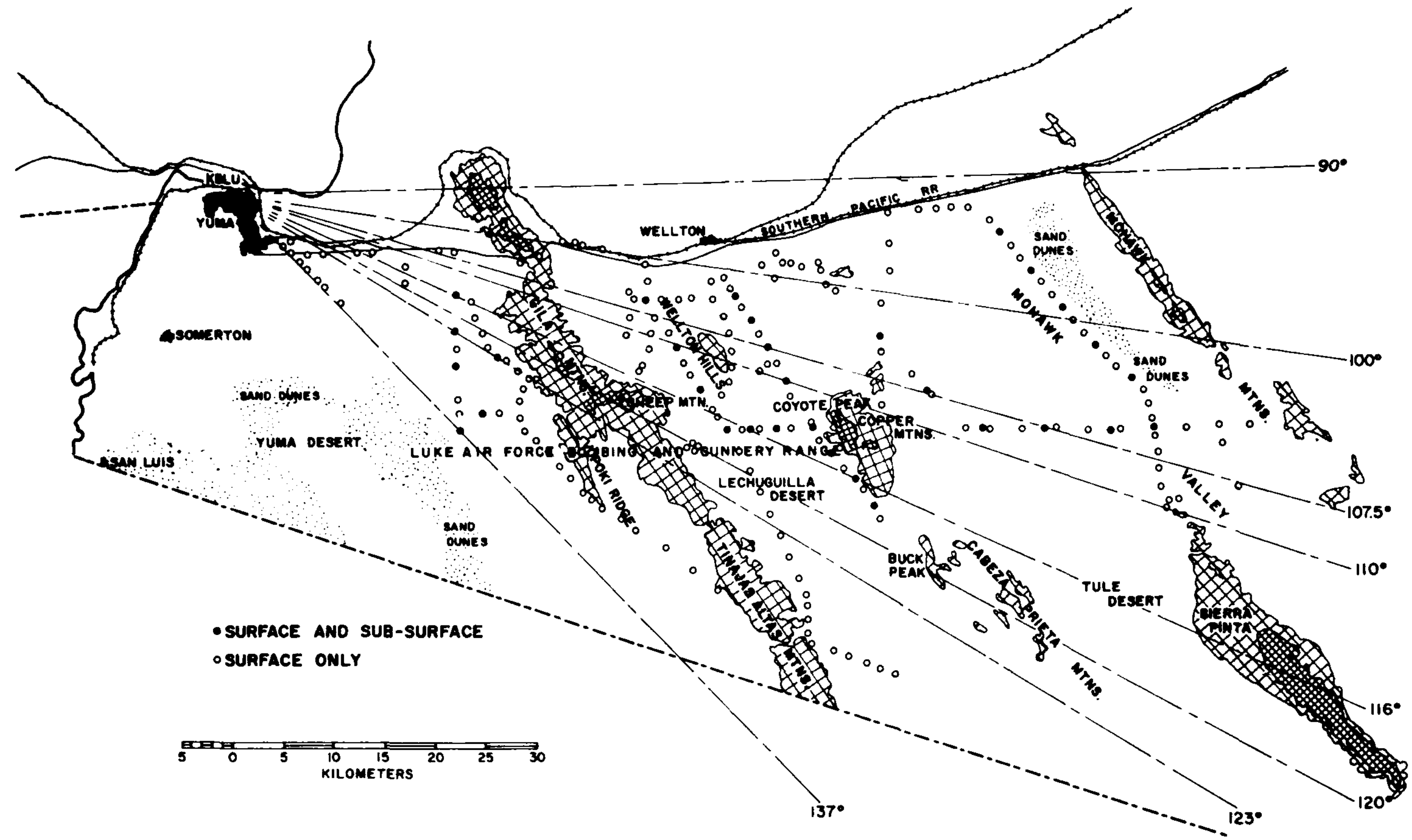

Figure 1. RADC Measurement Sites in the Yuma and Lechuguilla Deserts

and

$$p_e = |p_e| = \frac{\epsilon_o \omega k x}{2\sigma} .$$

$F(p_e)$ is the Sommerfeld propagation factor, p_e is the numerical distance, $\epsilon_o = 8.854 \times 10^{-12}$ F/m, ω is the radian frequency, σ is the surface conductivity (Siemens/meter) and kx is the distance in wavelengths. Eq. (1) can also be expressed

$$\log |E \cdot x| = \log |F| + \log 300 \sqrt{P} , \tag{2}$$

where log = $\log_{10}$. $|F|$ is plotted as a function of p_e on a logarithmic scale in Figure 2. For numerical distances of the order of unity or less,

$$\log |F| \simeq -0.183 \, |p_e| . \tag{3}$$

At 560 kHz, Eq. (3) is valid for distances out to at least 50 km if $\sigma = 0.01$ S/m and to 100 km for $\sigma = 0.02$ S/m. Combining Eqs. (2) and (3),

$$\log |E \cdot x| \simeq - \frac{0.0915 \, \epsilon_o \omega k}{\sigma} x + \log 300 \sqrt{P} . \tag{4}$$

Equation (4) is in the standard form $y = mx + b$, where, upon the application of linear regression analysis to the measured $|E \cdot x|$ data, the slope

$$m = -0.0915 \frac{\epsilon_o \omega k}{\sigma} \tag{5}$$

yields an estimate for σ, and the y-intercept

$$b = \log 300 \sqrt{P} \tag{6}$$

indicates an apparent radiated power

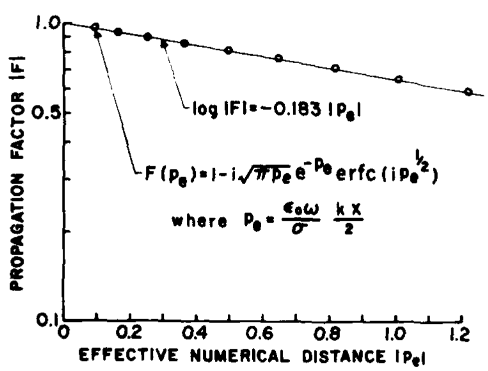

Figure 2. Amplitude of the Propagation Factor

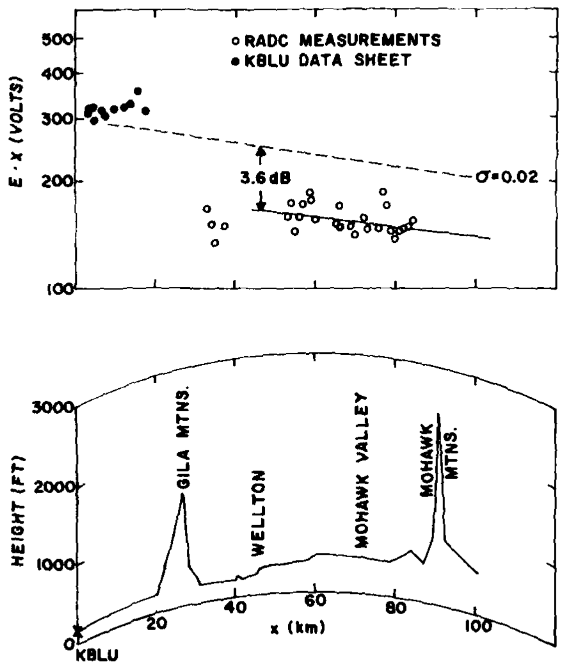

Figure 3. Southern Pacific RR (90° - 100°) Sector Path Profile (lower portion) and Signal Strength-Distance Product

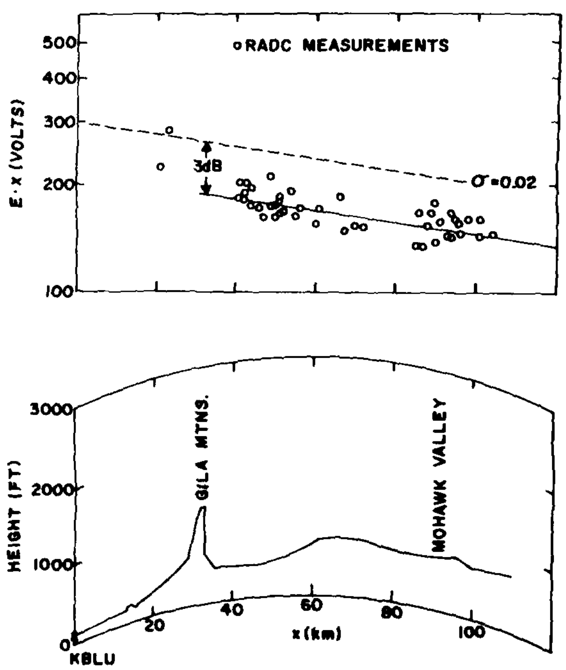

Figure 4. Mohawk Valley (100° - 107.5°) Sector Path Profile (lower portion) and Signal Strength-Distance Product

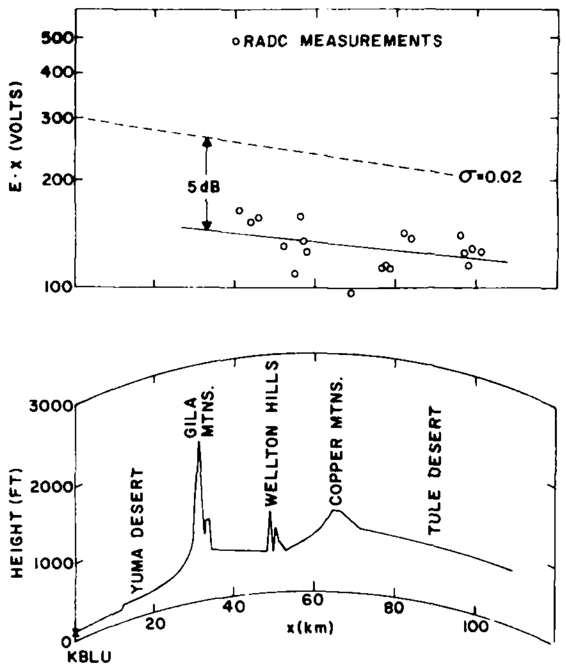

Figure 5. Wellton Hills (107.5° - 110°) Sector Path Profile (lower portion) and Signal Strength-Distance Product

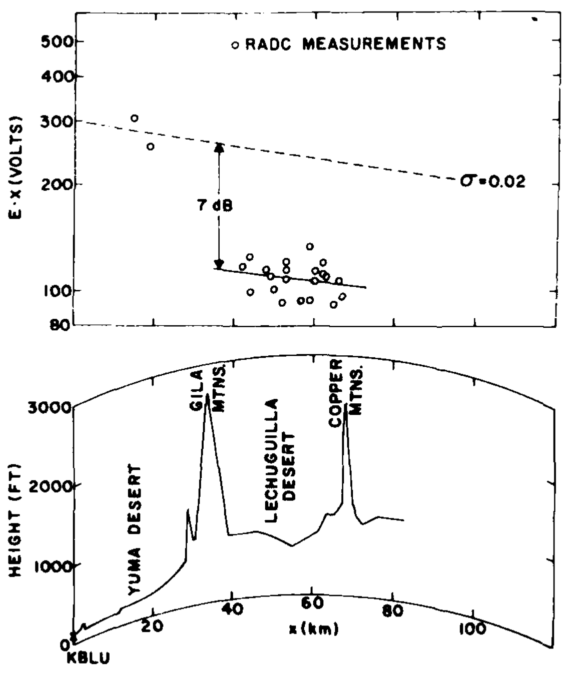

Figure 6. Coyote Peak (110° - 116°) Sector Path Profile (lower portion) and Signal Strength-Distance Product

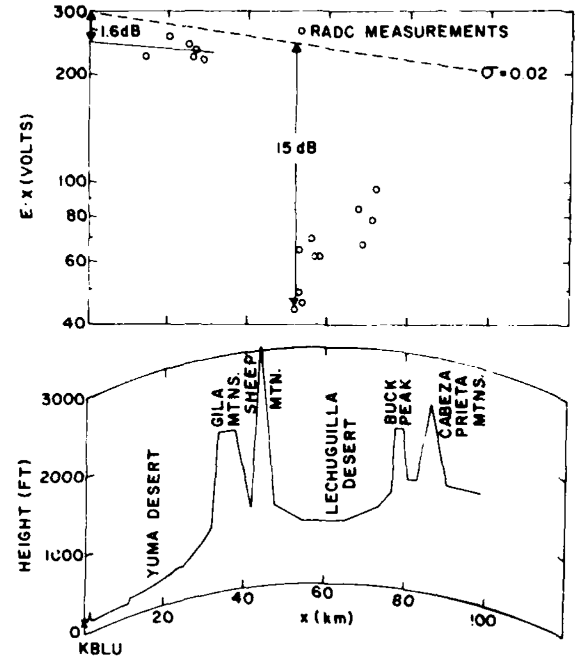

Figure 7. Sheep Mountain (116° - 120°) Sector Path Profile (lower portion) and Signal Strength-Distance Product

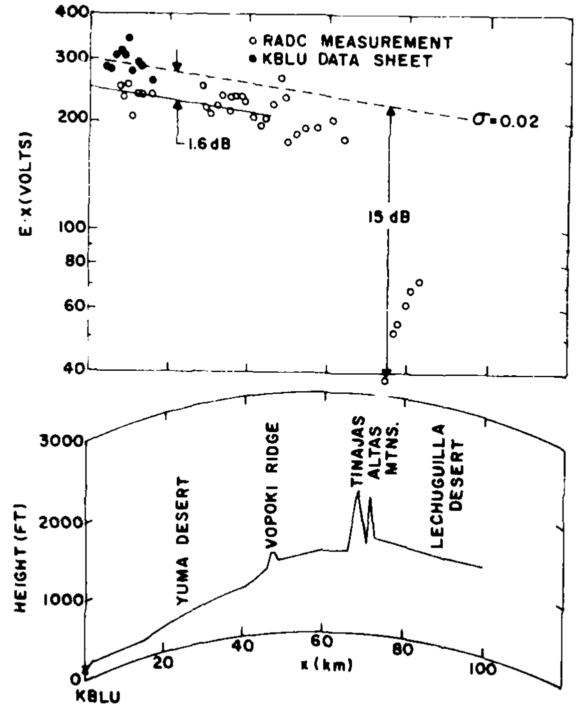

Figure 8. Tinajas Altas Mountains (123° - 137°) Sector Path Profile (lower portion) and Signal Strength-Distance Product

4. RESULTS OF REGRESSION ANALYSIS

4.1 Estimate of Conductivity

The upper portions of Figures 3 to 8 show measured values of $|E \cdot x|$ on a logarithmic scale vs distance from the KBLU antenna. The lower portions are corresponding terrain profiles which reveal long flat path segments occasionally interrupted by relatively steep ridges. The effective conductivity of these flat segments was estimated by fitting a regression line to selected data points not too close to the mountain ridges, and then using Eq. (5) to estimate σ. The regression line is shown in the figures as a solid line, and the σ estimates are given in Table 1. Assuming the data is normally distributed about the regression line, we can assign confidence limits[6] to the calculated values of σ. The results of choosing a 95 percent interval are shown in the last column of Table 1. Evidently only the 100° - 107.5° sector contained enough data over a sufficiently long and flat range to permit a reasonably accurate estimate for σ, which was 0.022 S/m. This value is somewhat higher than the 0.01 S/m estimated by Morgan[7] or the 0.008 S/m estimated by the FCC.[8]

Some of the data scatter within the flat segments was due to the fact that the measurements were not along radial paths, and each data point within a given sector actually represents propagation over a slightly different path. Additional perturbations were produced by local anomalies such as ore deposits, faults, power and telephone lines, and railroads, as well as by focussing, diffraction, and multipath effects.

Table 1. Estimated Effective Conductivity

Sector [Degrees]	No. Data Points	Correlation Coefficient	Est σ [S/m]	95% Conf. Limits [S/m]
90 - 100	24	0.39	0.023	*
100 - 107.5	44	0.70	0.022	0.016 - 0.033
107.5 - 110	19	0.42	0.029	*
110 - 116	21	0.22	0.026	*
116 - 120	6	0.22	0.030	*
123 - 137	20	0.52	0.023	0.011 - 0.122

*The data scatter was too great to permit an accurate determination of σ.

(Due to the number of references cited above, they will not be listed here. See References, page 20.)

4.2 Apparent Radiated Power

In Figures 3 to 8 the dashed lines plot $|E \cdot x|$ from Eq. (4) for a flat earth of conductivity 0.02 S/m from a 560 kHz transmitter radiating 1 kW. Regression analysis on RADC measured data over path segments where no mountain ridges are interposed between the transmitter and observer (for example, Figures 7 and 8) yields y-intercepts displaced approximately 1.6 dB below the equivalent 1 kW nominal value. This discrepancy could be due to the NM-25T calibration, since $|E \cdot x|$ data supplied by KBLU is consistently higher than the RADC measurements. On the other hand, beyond the Gila Mountains (Figures 3 through 6) the regression lines are displaced from 3 to 5 dB below the nominal 1 kW value. This reduction in apparent radiated power can be interpreted as the effect of the mountain ridge in extracting energy from the propagating ground wave.

The losses may be due to scattering by the terrain elevation changes and/or to increased absorption by a poorly conducting path segment, but neither mechanism can be adequately treated by flat earth theory. Indeed for certain paths the signal strength drops by as much as 15 dB behind the mountain ridges (Figures 6 and 7) and then exhibits a recovery effect with distance. Such a variation requires the more comprehensive theory which follows in the next section.

5. PROPAGATION OVER ROUGH, NON-HOMOGENEOUS TERRAIN

5.1 Hufford's Integral Equation

Calculations of the effects of irregular terrain can be made via a one-dimensional integral equation derived by Hufford.[9] His Eq. (11) in the notation of Figure 9 is

$$W(x) = 1 - \int_0^x W(s) \cdot f(s) \frac{ds}{\sqrt{s(x-s)}} \tag{7}$$

where W is the attenuation function for the Hertz potential. In terms of the vertical electric field, an approximate expression for W is

$$W \approx \left| \frac{E \cdot x}{\lim\limits_{x \to 0} E \cdot x} \right|$$

9. Hufford, G. A. (1952) An integral equation approach to the problem of wave propagation over an irregular terrain, Quart. J. Appl. Math. 9:391-404.

provided W is slowly varying. The quantity

$$f(s) = e^{-i\pi/4} \sqrt{\frac{kx}{2\pi}} \left[\delta + \frac{\partial r_2}{\partial n} \right] e^{ik(r_1 + r_2 - r_0)} ,$$

where δ is the (normalized) surface impedance

$$\delta = \sqrt{\frac{\epsilon_0 \omega}{\sigma}} \; e^{-i\pi/4} .$$

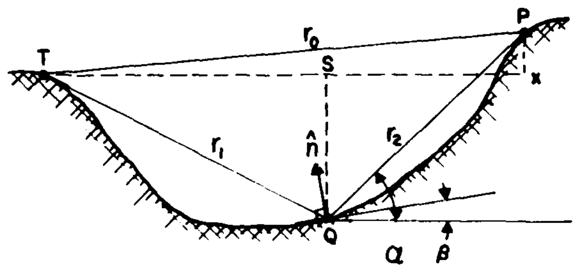

Figure 9. Geometry for the Integral Equation. s and x are the horizontal distances of the scattering point Q and the observer P, respectively, from the source T. α is the slope of r_2, β is the terrain slope at Q, and $\hat{n}$ is a unit vector at Q normal to the terrain

The factor $\partial r_2/\partial n$ takes into account the terrain slope and the aspect angle with respect to the observer. As may be seen from Figure 9,

$$\frac{\partial r_2}{\partial n} = \sin (\beta - \alpha)$$

where β is the terrain slope and α is the slope of r_2.

For gently undulating terrain with gradual inhomogeneities, the functions W(s) and f(s) are slowly varying. To the extent that W and f can be represented as constants within arbitrarily small intervals $\Delta s = s_n - s_{n-1}$, an approximate solution of Eq. (7) is

$$W_{n+1} \approx 1 - \sum_n W_n f_n I_n \tag{8}$$

where W_n is a constant value for W over the nth interval, f_n is a constant value for f over the same interval and

$$I_n = \int_{s_{n-1}}^{s_n} \frac{ds}{\sqrt{s(x-s)}} = \sin^{-1} \left[1 - \frac{2 s_{n-1}}{x} \right] - \sin^{-1} \left[1 - \frac{2 s_n}{x} \right] .$$

5.2 Numerical Solution for Special Cases

Equation (8) was solved numerically via a CDC 6600 computer for several cases. In Figure 10 the results of including a Gaussian-shaped ridge

$$G(x) = h \exp\left[-9 \left(\frac{x-b}{W}\right)^2 \right] \tag{9}$$

on an otherwise flat, homogeneous earth are shown for two values of conductivity. In Eq. (9), G(x) is the terrain elevation, h is the ridge height at x = b and w is the ridge width measured at $G(x) \cong h/10$. This form corresponds to the model chosen by Berry.[10] The attenuation function $|W|$ at first decreases at the flat earth rate, and then increases to a maximum just before the crest of the ridge. Behind the ridge there is a minimum, and then a partial recovery with increasing distance from the source.

Figure 11 illustrates the perturbation in $|W|$ caused by a 6 km wide segment of conductivity σ_s, centered at 30 km, in an otherwise homogeneous flat path of conductivity 0.02 S/m. Such a path represents the much poorer conductivity expected in the mountain ridges.[11] $|W|$ follows the flat earth attenuation rate out to the beginning of the segment, and then, depending on the selected value for σ_s, decreases more or less rapidly until the far edge of the segment is reached. As in the case of the ridge, $|W|$ partially recovers as the distance from the inhomogeneity increases. (The abrupt conductivity change in this model does not satisfy the conditions under which Eq. (8) was derived, so the results are not valid in the immediate vicinity of the edges of the segment.) A comparison of Figures 10 and 11 with 7 and 8 seems to show that the effect of a segment of poor conductivity more closely matches the observed $|E \cdot x|$ variation than the elevation effect. The models demonstrate that irregularities in both profile and earth conductivity play significant roles in determining the propagation of MF over ridges.

---

10. Berry, L. A. (1967) Radio propagation over a Gaussian-shaped ridge, IEEE Trans. Antennas Propag. AP-15(No. 5):701-702.
11. FAO-Unesco, Soil Map of the World, Vol. II, Unesco-Paris, 1974.

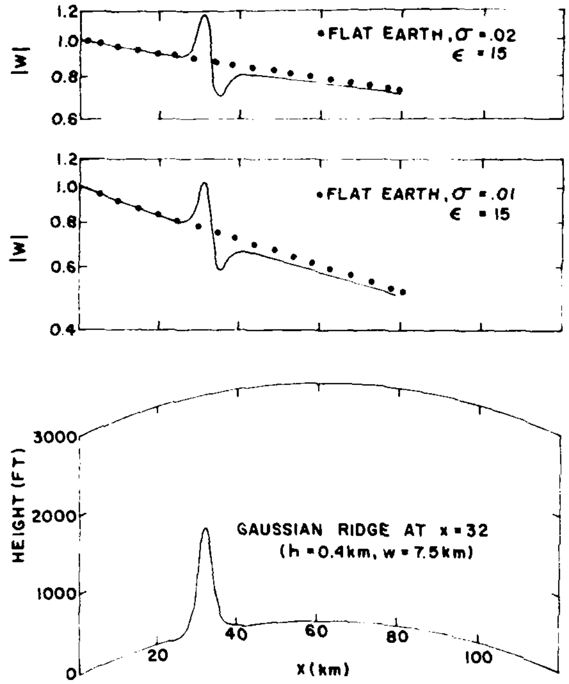

Figure 10. The Attenuation Function |W| on the Surface of the Ridge Shown at the Bottom of the Figure, for Two Values of Earth Conductivity

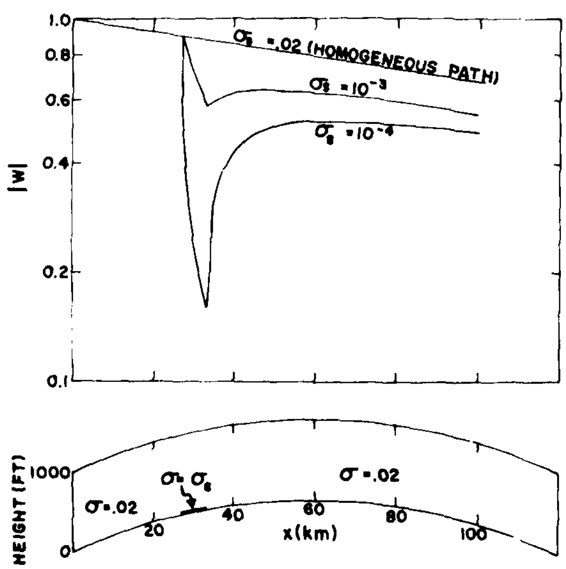

Figure 11. The Attenuation Function |W| on the Surface of the Inhomogeneous Path Shown at the Bottom of the Figure, for Three Values of σ_s

6. PENETRATION BELOW THE DESERT FLOOR

Attenuation of MF fields with depth in homogeneous, well-conducting soil is described by

$$H = H_o e^{-y/\delta_s} e^{-jy/\delta_s}$$

where H_o is the magnitude of the field at the surface, y is the depth below the surface and δ_s is the depth of penetration or skin depth. Attenuation measurements of the magnetic fields penetrating the desert soil were made by lowering a loop antenna into 18-in. diameter holes drilled approximately 6-ft deep by a commercial power auger, and recording the decibels change from the surface reading. An effective skin depth was then calculated via

$$\delta_s = \frac{8.69\, y}{H_o\,[dB] - H[dB]} \quad . \tag{10}$$

A total of 30 holes were drilled at various locations as indicated in Figure 1. The relative attenuation was read to within about ± 0.25 dB on the NM-25T panel meter, and the depth was measured accurately. The average skin depth calculated was 28.25 ft with a standard deviation of 13.09 ft.

7. DISCUSSION AND CONCLUSIONS

The data in this report can be used to estimate total propagation path loss for a point-to-point communication link between terminals buried in the desert southeast of Yuma and separated by mountain ridges. The desert valley soils have relatively high apparent conductivity, with a correspondingly low attenuation of propagating MF radio waves. The mountain ridges can have a large effect which depends on the location of the terminal. The mountains can be modeled to predict the attenuation, but good accuracy requires that both the terrain profile and the ground constants be known. An overburden of desert soil will result in additional loss.

The measurements and portions of the modeling work in this report were presented to an MX C^3 working group at a technical interchange meeting at Norton AFB, California on 14 December 1977.

References

1. Terman, F. E. (1943) Radio Engineer's Handbook, McGraw-Hill, New York.
2. Wait, J. R., and Campbell, L. L. (1953) Transmission curves for ground wave propagation at low radio frequencies, Radio Physics Laboratory Report R-1. Defence Research Telecommunications Establishment, Ottawa.
3. International Radio Consultative Committee (C.C.I.R.) (1974) Propagation in Non-Ionized Media (Study Group 5), Vol. 5, XIIIth Plenary Assembly, Geneva, 1974, International Telecommunication Union, Geneva, 1975.
4. Reference Data for Radio Engineers, 4th ed. (1956), ITT Corp., New York, p. 714 ff.
5. Reference Data for Radio Engineers, 5th ed. (1957) ITT Cprl., New York, p 741 ff.
6. Kreyszig, E. (1972) Advanced Engineering Mathematics, 3rd ed., Ch. 19, Wiley, New York.
7. Morgan, R. R. (1968) World-Wide VLF Effective Conductivity Map, Westinghouse Report 80133F-1, Westinghouse Electric Corp., Environmental Science and Technology Dept., Boulder, Colorado.
8. Fine, H. (1954) An effective ground conductivity map for continental United States, Proc. IRE 42:1405-1408.
9. Hufford, G. A. (1952) An integral equation approach to the problem of wave propagation over an irregular terrain, Quart. J. Appl. Math. 9:391-404.
10. Berry, L. A. (1967) Radio propagation over a Gaussian-shaped ridge, IEEE Trans. Antennas Propag. AP-15(No. 5):701-702.
11. FAO-Unesco, Soil Map of the World, Vol. II, Unesco-Paris, 1974.

MISSION
of
Rome Air Development Center

RADC plans and executes research, development, test and selected acquisition programs in support of Command, Control Communications and Intelligence (C^3I) activities. Technical and engineering support within areas of technical competence is provided to ESD Program Offices (POs) and other ESD elements. The principal technical mission areas are communications, electromagnetic guidance and control, surveillance of ground and aerospace objects, intelligence data collection and handling, information system technology, ionospheric propagation, solid state sciences, microwave physics and electronic reliability, maintainability and compatibility.

Printed by
United States Air Force
Hanscom AFB, Mass. 01731